J Mater Sci (2007) 42:9572–9581
DOI 10.1007/s10853-007-1748-x

INTERFACE SCIENCE

Reduction–adsorption behavior of platinum ions on activated carbon fibers

**Shuixia Chen · Ruimei Xu · Huixing Huang ·
Fenyun Yi · Xin Zhou · Hanmin Zeng**

Received: 1 September 2006 / Accepted: 6 April 2007 / Published online: 23 June 2007

Abstract A number of activated carbon fibers (ACF) were prepared by activation with steam, Phosphoric acid, or Zinc Chloride. Their reduction-adsorption behavior for Pt(IV) was studied using scanning electron microscopy, X-ray diffraction (XRD) and X-ray photoelectron spectroscopy. The results show that Pt ions in solution can be adsorbed by ACFs and reduced to metallic platinum. The reduction–adsorption capacity of ACF for Pt could be greater than 200 mg/g. Generally, higher specific surface area or lower electrode potential produces a higher capacity. Most of the adsorbed platinum ions were reduced into metallic platinum, and about 25% of platinum atoms remained as Pt(II) or Pt(IV). XRD examination showed that the Pt particles on the ACF surface were crystallized when heated to 673 K.

Introduction

The carbon-supported noble metal electrocatalyst on a gas diffusion electrode is a very important component for fuel cells; platinum is the most commonly used noble metal among these catalysts. To reduce the amount of Pt on the electrode, Pt is usually dispersed on carbon black supports by chemical [1] or electrochemical [2] reduction of Pt salts. The electrode performance and durability are closely related to electrode morphology, electrode wettability, as well as morphology and crystalline orientation of the noble metal particles [3–5].

High surface area carbon blacks used as effective solid supports for nanoscale noble metal dispersion can increase the electrode efficiency and reduce the cost of electrocatalysts [6]. In fuel cells, despite high surface areas of the electron-conducting carbon black support and the effective dispersion of Pt electrocatalysts, self-agglomeration of the carbon particles limits the approach of fuel and oxidant to the active sites, and therefore the electrocatalyst efficiency of the fuel-cell electrode will be weakened.

As we know, fibers offer flexibility which does not apply to the usual powdered or granular materials. Fibrous catalytic packs offer the advantages of an immobile catalyst and a short diffusion distance. Another advantage of fibrous catalysts is their low resistance to flow of liquid and gases through a bundle of fibers, which is lower than that of a powdered or granulated bed [7]. Thus, they can be used as an attractive alternative in fuel cell.

Activated carbon fibers (ACFs) have attracted a considerable attention because of their excellent adsorption properties for small molecules. The unique micropore distribution and high specific surface area make them be widely used in gas separation, solvent recovery, water purification, and some other environment fields. In addition to plentiful pores and high specific surface area, ACFs have plentiful surface chemical groups that make them highly reactive activity. Ever since reduction property of ACF was first reported in 1989 [8], many studies have been conducted on the reduction and adsorption of noble metal ions on ACF, the reaction mechanism, and the application in noble metal recovery and in antibacterial materials [9–11]. The reduction capacity of ACF is determined by the electrode potential of the metallic ion pairs and the chemical

---

S. Chen (✉) · R. Xu · H. Huang · F. Yi · X. Zhou ·
H. Zeng
Key Laboratory of Polymeric Composite and Functional
Materials of Education Ministry, Materials Science Institute,
School of Chemistry and Chemical Engineering,
Zhongshan University, Guangzhou 510275, China
e-mail: cescsx@mail.sysu.edu.cn

properties of ACF. The favorable reduction ability of ACF for platinum ions may provide another method for the preparation of platinum electrocatalyst for proton exchange membrane fuel cell (PEMFC).

In order to control the particle size and distribution of platinum on carbon and to improve the electrocatalytic efficiency, many experiments have been done in the preparation of Pt/C catalysts. It was reported that Pt nanoclusters were supported on carbon black and CNT by alcohol-reduction method in presence of a surfactant, which allow a significant improvement of the electrocatalytic performance in hydrogen oxidation at the anode [12]. Platinum and palladium nanoparticles have also been supported on Vulcan XC-72 carbon by a microwave-assisted polyol process. The average particle size of Pt and Pd nanoparticles was reported to be 4 and 5 nm, respectively. High power density could be yielded using Pt/C as the anode catalyst prepared by this method [13]. We also used the intermittent microwave heating technique to support Pd nanoparticles on different types of the carbon materials including multiwall carbon nanotube, carbon black and activated carbon fiber, the results showed the significant influence of support on the catalytic activities of the Pd-based electrocatalysts for ethanol oxidation [14]. In order to control the size and loading level, nanoclusters supported on carbon were prepared by chemical method of Pt precursor reduction onto chemically treated carbon blacks (CBs). It was reported that base-treated CBs-supported Pt showed the smallest particle size of 2.65 nm and the highest loading level of 97% among the chemical-treated CBs-supported Pt catalysts [15]. Single-wall carbon nanohorns (SWNHs) were also used to support platinum catalyst by using a colloidal method. It was reported that the Pt particles were homogeneously dispersed on the SWNHs, and their particle size was about 2 nm. This size was less than half of that supported on conventional carbon black. A fuel cell using the SWNHs had a larger current density than one using the carbon black [16].

In this paper, the reduction adsorption behavior of ACFs for platinum ion, factors that may affect the reduction capacity and the adsorption kinetics have been studied. Technique that would enhance the reduction–adsorption and control the distribution of the adsorbed platinum particles was primarily discussed.

Experimental

Preparation of ACF

A vegetable fiber–Sisal fiber was impregnated in 5% NaOH solution for 24 h to remove pectin and other impurities, then impregnated with 35 vol.% H_3PO_4 or 35 wt.% $ZnCl_2$ solution for 24 h. The pretreated fiber was heated under inert atmosphere to 600–900 °C and then kept at that temperature for 0–120 min for carbonization and activation; activated carbon fibers prepared with phosphoric acid (HPSACF) or zinc chloride (ZCSACF) activation were thus obtained. Another part of sisal fiber treated with NaOH was directly heated to 850 °C under inert atmosphere for carbonization, and then activated with steam at the same temperature for 15–120 min., the resulted activated carbon fiber was noted as SACF.

The preparation method of viscose based activated carbon fiber (VACF) is similar to the method for SACF. Granular active carbon (AC) is a commercial product; the product re-activated with zinc chloride was noted as ZCAC.

All ACFs and ACs were washed with diluted HNO_3 and then with deionized water till neutral pH of effluent solution before they were used in the adsorption of Pt ions and structure characterization.

The pore parameters of some typical samples are listed in Table 1, where S_{BET}, S_{micro} are total surface areas and micropore surface area of carbon, respectively; V_t and

Table 1 Pore structure parameters of ACFs

	S_{BET} (m^2/g)	S_{micro} (m^2/g)	V_t (m^3/g)	V_{micro} (m^3/g)	D (nm)
SACF15	932.3	799.9	0.452	0.374	1.94
SACF30	1379.2	681.6	0.698	0.298	2.02
SACF60	871.4	179.1	0.635	0.070	2.91
ZCSACF650	1198.7	1003.1	0.570	0.467	1.90
ZCSACF750	1203.8	974.3	0.577	0.453	1.92
ZCSACF850	1362.2	913.6	0.654	0.422	1.92
ZCSACF900	948.9	819.8	0.449	0.380	1.89
HPSACF700	94.4	84.7	0.049	0.004	2.00
HPSACF800	552.3	446.7	0.265	0.208	1.92
HPSACF850	977.5	628.9	0.463	0.287	1.89
HPSACF900	1158.6	881.4	0.551	0.409	1.90

V_{micro} are total pore volume and micropore volume; D is the average width of total pore. The numbers in the given abbreviations represent the activation time or activation temperature. For SACF series, the numbers represent the activation time, that is, the samples were activated at 850 °C for 15–60 min. For ZCSACF and HPSACF series, the numbers represent the activation temperature, that is, the samples were activated for 90 min at the temperature of 650–850 °C.

Adsorption of platinum

Certain weight of ACF, dried at 380 K in vacuum, was added into the solution containing 200–1,000 mg/L Pt(IV). After shaking with the Pt(IV) ion solution at 298 K for 24 h, ACFs were filtered. The concentration of Pt ions in solution before and after adsorption was measured by atomic absorption spectrophotometry. The static adsorption amount of Pt on ACF was calculated by the following formula:

$$q = \frac{(C_0 - C)V}{m_{\text{ACF}}}, \qquad (1)$$

where q is the adsorption amount of Pt on ACF (mg/g); C_0 and C are the concentrations of Pt ion in solution before and after adsorption (mg/L); V is the solution volume (L); m_{ACF} is the weight of ACF (g).

For dynamic adsorption, the residual concentration of Pt ions in solution was analyzed at regular intervals.

Determination of electrode potential of ACF

The working electrode was prepared by sticking a single filament of ACF onto a copper wire; saturated calomel electrode and Platinum electrode were used as reference and counter electrodes, respectively. The electrode potential of ACF was measured in 0.01 mol/L potassium chloride solution using a VoltaLab 80 (PGZ402 & VoltaMaster 4) Universal Electrochemical Laboratory.

Structure characterization

A RigaRu D/MAX-IIIA X-ray diffractometer was used to study the crystalline structure of platinum and ACFs. An Escablab MK II X-ray photoelectron microscope (XPS) was used to analyze the surface chemical structure. Nitrogen adsorption isotherms measured at 77 K using an ASAP 2010 volumetric adsorption apparatus from Micromeritics (Norcross, GA, USA) were used to characterize the pore structure of ACFs. A JSM-6330F scanning electron microscope (SEM) was used to observe the surface structure of ACF and the distribution of platinum particles.

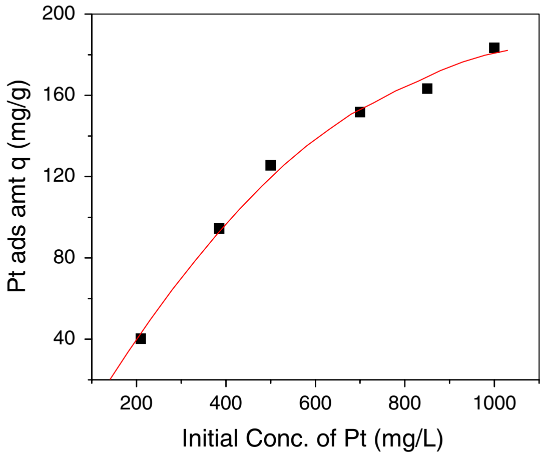

Fig. 1 Effect of Pt initial concentration on Pt adsorption capacity on ACF

Results and discussion

Pt adsorption capacity on ACF

Figure 1 shows the curve of Pt adsorption amounts on SACF at 303 K vs. the initial Pt(IV) concentration in solution. Pt adsorption amount increases from 40 to over 180 mg/g when the initial Pt concentration increases from 200 to 1,000 mg/L, which reveals a close correlation between Pt adsorption capacity and the Pt(IV) concentration in solution. Based on tendency of the curve in Fig. 1, Pt adsorption on ACF has not yet achieved its maximum capacity; the adsorption amount will still increase with increasing Pt(IV) concentration in solution.

Table 2 shows the comparison of Pt adsorption capacity on ACFs prepared by different activation methods. Although these three kinds of ACF have similar specific surface area (about 1,200 m^2/g), their adsorption capacities for Pt(IV) are quite different. At the same condition, the Pt adsorption capacity of ZCSACF prepared by $ZnCl_2$

Table 2 Adsorption amounts of $PtCl_6^{2-}$ on carbon prepared by various methods

Sample	SACF	ZCSACF	HPSACF	SCF	AC
S_{BET} (m^2/g)	1250.5	1203.8	1158.6	262.5	831.0
Q (mg/g)	90.19	88.81	47.06	33.0	82.67

$C_0 = 210$ mg Pt/L, pH = 2.36

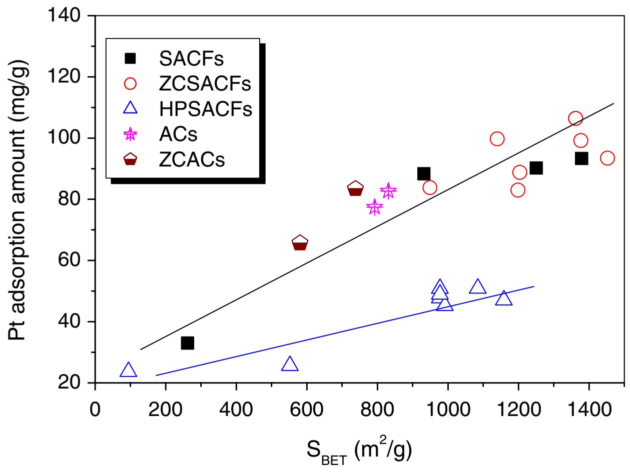

Fig. 2 Platinum adsorption amount on active carbon as a function of surface area

activation, and SACF prepared by steam activation, is two times of the capacity of HPSACF prepared by phosphoric acid activation. This is obviously different from the silver adsorption performance on these ACFs. Our previous experimental results indicated that the reduction–adsorption capacity of HPSACF for $Ag(NH_3)_2^+$ was much higher than that of SACF or ZCSACF [9, 11].

The Pt adsorption amount on commercial AC re-activated with steam is also listed in Table 2. It is obvious that this AC also has higher adsorption capacity for platinum.

A quite interesting phenomenon is that sisal based carbon fiber (SCF), which has very low specific surface area, can also adsorb certain amount of Pt. Apparently, adsorption of Pt on ACF is determined not only by its specific surface area, but also by its surface chemical properties. In fact, on the surface of SCF, there are certain reactive groups such as hydroxyl and carbonyl groups, which contribute to the adsorption and reduction of platinum ion on SCF.

Figure 2 presents the data of Pt adsorption on ACFs prepared by different methods, and plots the adsorption amount of Pt on ACF as the function of specific surface area. Data of Pt adsorption on granular active carbon activated with zinc chloride (ZCAC) are also presented on this figure. The results reveal a positive correlation between the adsorption amount of Pt and the specific surface area of ACF. Pt adsorption capacity of ACF increases linearly with ACF surface area. Obviously, higher surface area provides more places for the adsorption of platinum ions; at the same time, there are much more chemical groups on ACF with increasing specific surface area, these chemical groups will be propitious to enhance the static adsorption of platinum.

Data in Fig. 2 can be plotted as two linear curves with different slopes. One is for the adsorption of ACs and ACFs activated with steam or zinc chloride; it has steeper slope than the other one, which means the adsorption capacities on these kinds of ACFs or active carbon are more sensitive to their specific surface area; the other linear curve with less steep slope is for HPSACF activated with phosphoric acid, which would indicate the Pt adsorption capacity on this kind of ACF is less sensitive to surface area.

Obviously, the chemical properties of ACFs activated with different methods are quite different, thus their platinum adsorption ability will also different although they have similar specific surface area. In other words, Pt adsorption capacity of ACF is determined not only by its specific surface area but also by its surface chemistry. As one of the example, experiments of the influence of pH on Pt adsorption capacity showed that the Pt ion adsorption amount on SACF decrease from 90 to 75 mg/g with the increase of solution pH from 2 to 12. From the point of view of ion exchange, ACF act as a kind of weak acid adsorbent [17], the carboxyl group and phenol hydroxyl group will become positively charged at acidic condition, which will be in favor of the adsorption of $PtCl_6^{2-}$ ions [15]. On the other hand, Pt adsorption on ACF is a comprehensive process including adsorption, ion exchange, reduction–oxidation reaction, and some other interactions. In fact, the Pt adsorption capacity is an overall result of these interactions.

Morphology and distribution of Pt adsorbed on ACF

Figure 3a–d are SEM micrographs of HPSACF or ZCSACF before and after Pt adsorption. It is obvious that there are some platinum particles adsorbed on the surface of HPSACF and ZCSACF after contacting with Pt(IV)-containing solution, however these platinum particles are not well distributed on the surface. Figure 3e, f show SEM micrographs of SACF contacted with platinum solution for different period of time. The comparison of these two micrographs indicates that more platinum ions have been adsorbed and reduced onto the surface of SACF with the increase of adsorption time from 12 to 36 h.

Figure 4 shows SEM micrographs of VACF before and after Pt adsorption. It can be observed that a few Pt particles distribute on ridge of VACF (Fig. 4b). On the surface of those ZCVACF (Viscose based ACF activated with zinc chloride), there are much more platinum particles which are well distributed on ACF surface.

All of above micrographs evidently indicate that ACF can effectively adsorb platinum ions onto its surface and reduce them into metallic particles.

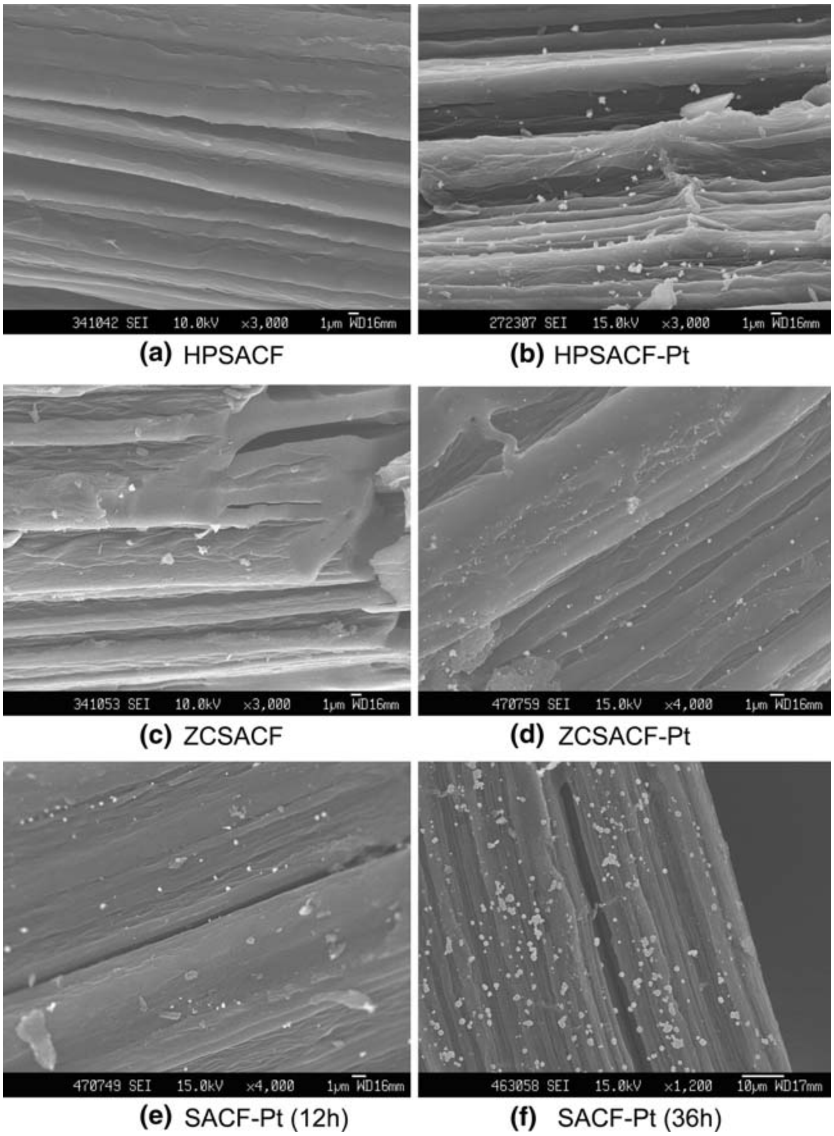

Fig. 3 SEM micrographs of sisal based ACF after adsorbing $PtCl_6^{2-}$. (**a**) HPSACF, (**b**) HPSACF-Pt, (**c**) ZCSACF, (**d**) ZCSACF-Pt, (**e**) SACF-Pt (12 h), (**f**) SACF-Pt (36 h)

Figure 5 shows the XRD pattern of SACF adsorbing Pt. The experimental results show that no diffraction peak of SACF adsorbing Pt can be identified (a in Fig. 5), however sharp diffraction peaks of crystalline platinum metal can be evidently observed after a heat treatment at 673 K of this sample (b in Fig. 5). It can be concluded that before heat treatment, there is very few metallic platinum particles on SACF, or platinum particles adsorbed on SACF is not well crystallized. The heat treatment would facilitate the reduction and crystallization of platinum ions on carbon surface. Same phenomenon was observed for ZCSACF, HPSACF, VACF, and AC: Pt diffraction peaks could only be observed after heat treatment of the carbon samples.

Calculation based on the XRD pattern using Scherrer equation indicates that the crystallite size of platinum particles on carbon after heat treatment at 675 K is about 11–22 nm. The results would indicate that the heat treatment will lead to the re-crystallization of Pt to form much bigger particles, which would be avoided in the preparation of Pt/C catalyst for fuel cell (Table 3).

Figure 6 shows XPS spectrum of Pt on SACF. The peak processing divides the spectra into two groups of twin peaks. According to reference [18, 19], one of the twin peaks at lower binding energy (72.5 and 75.5 eV) belongs to metallic platinum Pt(0), and the other at higher binding energy (73.8 and 76.8 eV) belongs to Pt(II) or Pt(IV). The comparison of the intensity of the two groups of twin peaks reveals that most of platinum ions adsorbed onto SACF have been reduced into metallic platinum, and about 25% of platinum atoms remain as Pt(II) or Pt(IV). Similar XPS spectra of Pt_{4f} for other porous carbon (ZCSACF, HPSACF, VACF or AC) that have adsorbed Pt can also be observed.

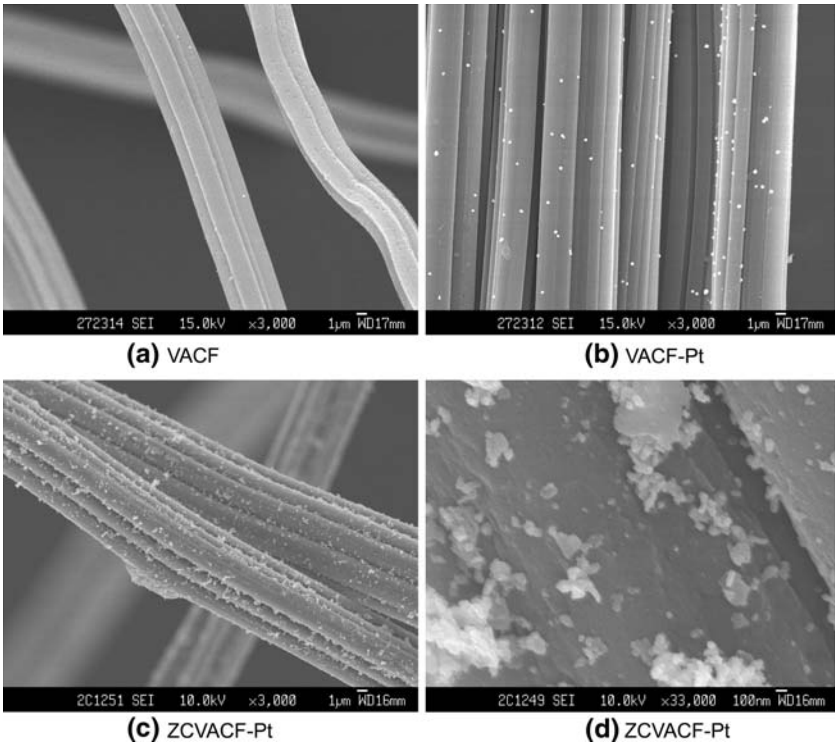

(a) VACF **(b)** VACF-Pt

(c) ZCVACF-Pt **(d)** ZCVACF-Pt

Fig. 4 SEM micrographs of viscose based ACF after adsorbing $PtCl_6^{2-}$. (**a**)VACF, (**b**)VACF-Pt, (**c**) ZCVACF-Pt, (**d**)ZCVACF-Pt

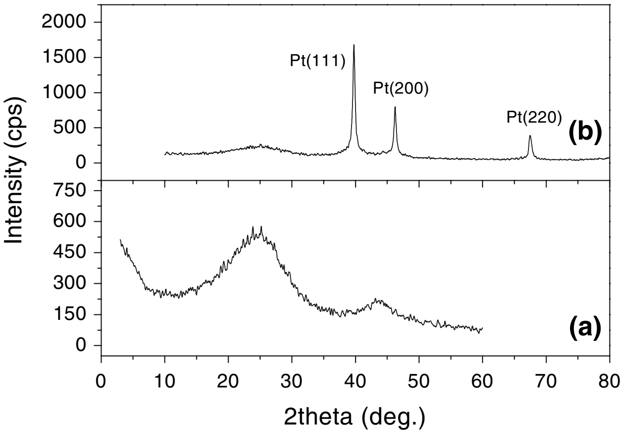

Fig. 5 X-ray diffraction patterns of SACF after adsorbing $PtCl_6^{2-}$. (**a**) Unheated, (**b**) heated for 4 h at 673 K

The relative proportion of Pt(0) and Pt(II, IV) on ACFs is estimated based on the Pt_{4f} peak processing (Table 4). The data in Table 4 indicate that over 75% of platinum has been reduced into metallic Pt, and about 25% of Pt remains in higher valence. However, it must be aware of the fact that data based on XPS spectrum would only represent the situation on the outside surface of carbon.

Table 5 shows the desorption results of platinum ions, in which Pt ions were desorbed by washing porous carbon with 0.1 M hydrochloric acid. If platinum on the surface of ACF still remains as its complex ion $PtCl_6^{2-}$, the un-reduced complex ions could be desorbed from ACF by HCl solution. However, the reduced metallic platinum is difficult to be dissolved and washed down by diluted HCl solution. The results in Table 5 reveal that part of platinum on ACF

Table 3 Crystallite size of Pt on porous carbon after heat treatment

Sample	Ads amt (mg/g)	L_a average (nm)
SACF-Pt	90	20.6
HPSACF-Pt	47	22.2
ZCSACF-Pt	89	17.4
VACF1510-Pt	57	11.3

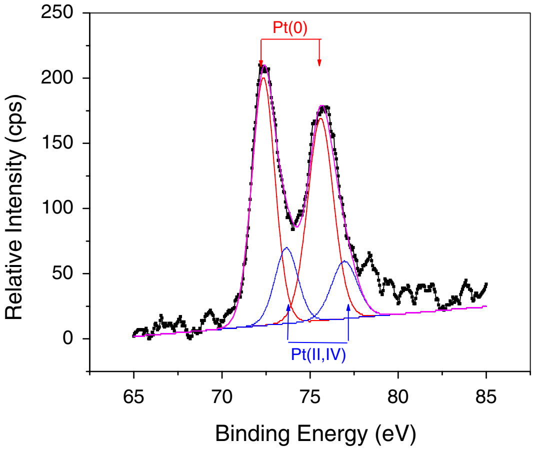

Fig. 6 XPS spectra of Pt_{4f} on SACF surface

Table 4 XPS peak processing results of Pt_{4f} on ACFs

	Total ads amt (mg/g)	Pt(0) @BE = 72.5 eV (at.%)	Pt(II, IV) @BE = 73.8 eV (at.%)
SACF	45.71	76.61	23.39
ZCSACF	50.07	77.75	22.25
VACF	37.75	74.60	25.40
AC	40.26	74.98	25.02

Table 5 The desorption amount of Pt(IV) from ACFs by 0.1 M HCl

Sample	Adsorption amount (mg/g)	Desorption percentage (%)	Sample	Adsorption amount (mg/g)	Desorption percentage (%)
SACF	88.28	19.8	VACF	89.35	16.0
ZCSACF	88.74	15.1	AC	77.46	21.7
HPSACF	50.8	31.9	SCF	33.0	79.9

really can be washed off by diluted HCl solution. Among these porous carbons, desorption percentage of platinum from SCF is the highest (79.9 wt.%). The desorption percentage of Pt from HPSACF, ZCSACF, VACF, SACF and AC is between 15 and 20%. These results are consistent with the results based on XPS peak processing (Table 4) on the whole, and may indicate that carbon fiber SCF has weaker reduction ability for Pt(IV) than active carbon or activated carbon fibers. The lower adsorption amount and lower reduction percentage of Pt on SCF would be due to its lower specific surface area and lower chemical group contents.

All of above results, including XPS, XRD, and desorption experiment, indicate that the adsorption of $PtCl_6^{2-}$ on ACF is comprised of physical adsorption, ion exchange, and the reduction reaction of platinum ions with carbon. The adsorption of Pt ions on ACF is quite different from the adsorption of Au ions. Because of the instability of Au(I) and higher electrode potential of $AuCl_4^-/Au$ (1.45V), Au(III) can be easily reduced into metallic gold. However, value of the electrode potential of $PtCl_6^{2-}/PtCl_4^{2-}$ and $PtCl_4^{2-}/$ Pt are only 0.68 and 0.755 V, respectively, and Pt(II) can exist in stable state in aqueous solution or form a stable complex, all of these factors cause the uncompleted reduction of platinum ion on ACF.

Dynamic adsorption and adsorption equilibrium

Figure 7 shows the dynamic adsorption amount of $PtCl_6^{2-}$ on ACF or AC as the function of time. The adsorption speed curves (differentiating the adsorption amounts by time) are showed in the right side of Fig. 7. It is obvious that the maximum adsorption amounts of Pt on various ACFs or AC is different when adsorption equilibrium was achieved. Among all these porous carbon, ZCSACF has the highest equilibrium adsorption capacity (more than 100 mg/g), and HPSACF is the lowest (less than 50 mg/g) at the same reaction condition. Based on the differential curves, ZCSACF and SACF have much faster adsorption speed than HPSACF and AC in the beginning period (0–100 min), which may indicate that ZCSACF and SACF have much stronger ion exchange ability than the other two adsorbents in this period. The adsorption speeds of platinum ions onto ZCSACF and SACF then decrease with time, and their adsorption equilibrium is

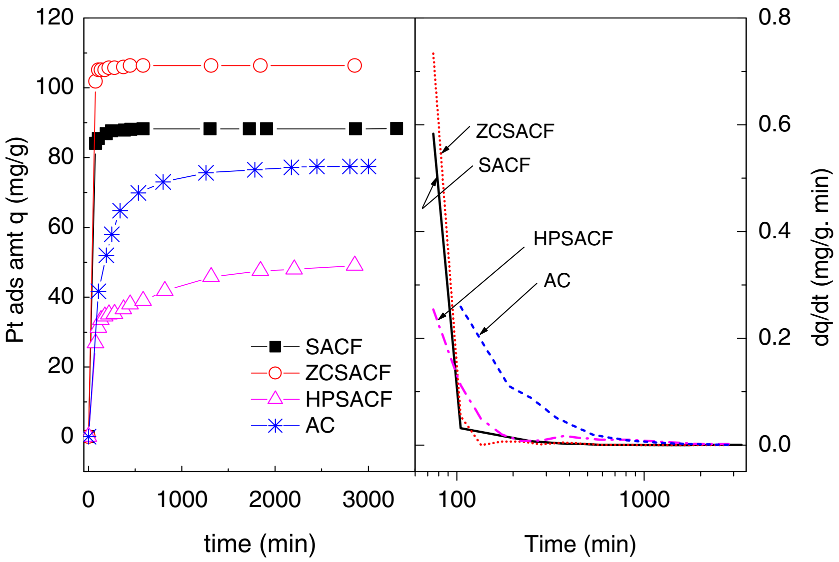

Fig. 7 Dynamic adsorption curves of $PtCl_6^{2-}$ onto ACFs and AC (303 K, C_0 = 385 mg Pt/L, pH = 3)

Table 6 Electrode potential values of different ACF and their Pt adsorption capacity

Activation temperature	SACF		ZCSACF		HPSACF	
	E (V)	q (mg/g)	E (V)	q (mg/g)	E (V)	q (mg/g)
1,023 K			0.464	87.11	0.579	59.60
1,123 K	0.444	78.13	0.434	86.20	0.599	37.90
1,173 K			0.594	83.43	0.594	61.20

achieved in about 150 min. The adsorption speed of platinum onto HPSACF is slower than onto ZCSACF and SACF, and the adsorption equilibrium of HPSACF for platinum will take about 2,000 min. Adsorption of platinum onto AC shows a very different characteristic, the adsorption speed of AC for platinum is much slower than those of the three ACFs, and it slowly decreases in the period of 100–1,000 min, which may be due to the lower diffusion speed of platinum ions onto AC.

Therefore, the adsorption of platinum onto porous carbon could be divided into three periods with different adsorption speeds. (1) Fast adsorption period. It occurs at the first 100 min. Because of the higher specific surface area and external surface area of ACF, platinum ions can easily diffuse and be adsorbed onto the micropores surface of ACF. At the very beginning of this period, the adsorption speed reaches the maximum, then it decreases with time. At this period, the adsorption amount increases quickly with time. (2) Slow adsorption period. At this period, the adsorption amount of platinum on porous carbon increases gradually with time, and the adsorption speed gradually decrease. The main reaction in this period would be the reduction of $PtCl_6^{2-}$ by carbon. (3) At the third period, most of the active surface of porous carbon is occupied by platinum ions; the adsorption and reduction tend to achieve equilibrium. The apparent adsorption speed will approach zero in this period, and the adsorption amount will approach its maximum. All ACFs have their similar first fast adsorption period. AC only experience the second and the third period.

Mechanism of reduction and adsorption of ACF for platinum ion

Effect of ACF electrode potential on its reduction–adsorption

The difference on the Pt adsorption amount and speed of ACFs prepared by different methods is closely related to their surface chemical properties that will determine their electrode potentials.

Considering the oxidation of surface carbon of ACF and the reduction of platinum as a galvanic cell, the two electrode reactions can be expressed as following:

$$\text{Anode}:\ [\mathrm{ACF}]_R + m\,H_2O \longrightarrow [\mathrm{ACF}]_O + nH^+ + n\,e \qquad (2)$$

$$\text{Cathode}:\ \mathrm{Pt(IV)} + n\,e \longrightarrow \mathrm{Pt(II,0)}, \qquad (3)$$

where the subscript R and O represent the reductive state and oxidative state of ACF. And the oxidation–reduction potential is:

$$E = E_{\mathrm{cathode}} - E_{\mathrm{anode}} = E_{\mathrm{Pt}} - E_{\mathrm{ACF}}. \qquad (4)$$

Because the potential of cathode (Pt) is a known value, the oxidation–reduction potential is determined by the potential of anode (ACF). The lower the anode potential is, the greater the potential difference of cathode and anode will be, and the more easily the electrode reaction will take place. The standard electrode potential values of some reactions of platinum are listed in following:

$$[PtCl_6]^{2-} + 2e \rightarrow [PtCl_4]^{2-} + 2Cl^- \qquad E^0 = 0.68\ \mathrm{V}$$
$$[PtCl_4]^{2-} + 2e \rightarrow Pt + 4Cl^- \qquad E^0 = 0.755\ \mathrm{V}$$
$$Pt(OH)_2 + 2e \rightarrow Pt + 2OH^- \qquad E^0 = 0.14\ \mathrm{V}.$$

Table 6 shows the electrode potentials (E) of ACFs prepared at different activation temperature and their Pt adsorption capacities (q). The results in Table 6 indicate that SACF and ZCSACF have similar electrode potential, ca. 0.45 V; and the electrode potential of HPSACF (over 0.55 V) is higher than those of the former two ACFs. As we know, $E_{PtCl_6^{2-}/PtCl_4^{2-}} = 0.68$ V, $E_{PtCl_4^{2-}/Pt} = 0.755$ V, and they are all higher than the electrode potential of the above three ACFs, which means that the reduction reaction of Pt ion and the oxidation of ACF can spontaneously take place. Because the potential difference of cathode E_{Pt} and anode E_{SACF} or E_{ZCSACF} is greater than the difference of E_{Pt} and E_{HPSACF}, SACF and ZCSACF will have higher reduction ability than HPSACF, which is consistent with the adsorption capacities of these ACFs for Pt.

The XPS comparison of chemistry structure of SACF surface before and after adsorbing Pt(IV)

Figure 8 shows the XPS spectrum of C_{1s} of SACF before and after Pt adsorption. It is evident that the asymmetric

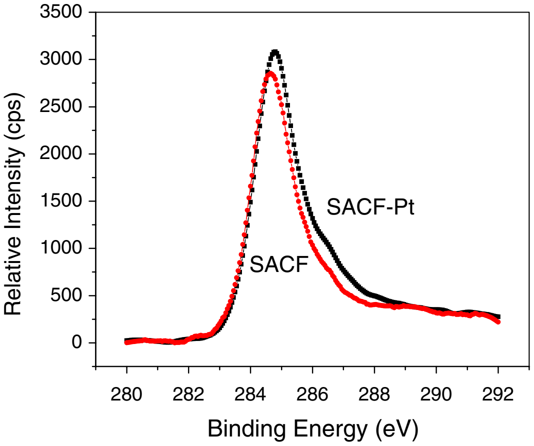

Fig. 8 XPS spectra of C_{1s} on SACF before and after adsorbing Pt(IV)

Table 7 XPS peak processing results of C_{1s} on SACF before and after adsorbing Pt(IV)

	Groups	BE (eV)	Percentage (atomic %)
SACF	C–H	284.67	71.09
	C–O	286.17	17.81
	C=O or O–C–O	287.75	5.84
	COOH	289.30	5.26
SACF-Pt	C–H	284.77	68.08
	C–O	286.20	21.74
	C=O or O–C–O	287.60	6.33
	COOH	289.10	3.85

spectrum of C_{1s} with a shoulder peak at higher binding energy became broadening after the Pt adsorption. The C_{1s} spectrum was resolved into four components representing graphitic carbon (BE = 284.5 eV), hydroxyl (phenolic) group (BE = 286 eV), carbonyl group (BE = 287.5 eV), and carboxyl group (BE = 290 eV). The molar percentages based on this peak processing results are presented in Table 7. The results in Table 7 evidently indicate that both the total oxygen-containing groups and the relative contents of hydroxyl group and carbonyl group increase after the Pt adsorption, which means the surface carbon on SACF was oxidized into higher valence groups such as hydroxyl or carbonyl groups when Pt(IV) ions were reduced.

According to the above results, the reduction–oxidation reaction mechanism could involve the following two reactions: The surface C–H was first oxidized into C–OH:

$$-\mathrm{C}-\mathrm{H}+\mathrm{Pt(IV)}+\mathrm{H_2O}\longrightarrow-\mathrm{C}-\mathrm{OH}+\mathrm{Pt(0,II)}+\mathrm{H}^{+}. \quad (5)$$

Some of the hydroxyl groups were further oxidized into carbonyl groups, and then the carbonyl groups were oxidized into carboxyl groups, which are not stable and could be decarboxylated to form a new C–H. a

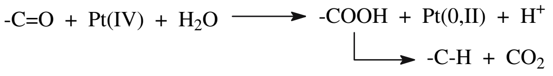

$$\text{-C=O} + \mathrm{Pt(IV)} + \mathrm{H_2O} \longrightarrow \text{-COOH} + \mathrm{Pt(0,II)} + \mathrm{H^+} \longrightarrow \text{-C-H} + \mathrm{CO_2} \quad (6)$$

Conclusion

(1) ACF can adsorb certain amount of Pt ions onto its surface and then reduce them into metallic platinum. The adsorption capacities of Pt on ACF are determined by the pore structure and surface chemistry of ACF. The adsorption capacity increases with the specific surface area of ACF, and decreases with the electrode potential of ACF. ACFs prepared by steam or zinc chloride activation have lower electrode potential than HPSACF, thus have higher ability than HPSACF to reduce Pt ions.

(2) The adsorbed Platinum is distributed as amorphous particles on the surface of ACF, and it can be crystallized when heated to 673 K.

(3) The adsorption process of platinum on porous carbon could be divided into three periods: initial fast adsorption, slow adsorption, and equilibrium adsorption. The fast adsorption of Pt on ACF may be due to high specific surface area and external surface area of ACF.

(4) The surface C–H is first oxidized into C–OH, then some of the hydroxyl groups are oxidized into carbonyl groups when Pt(IV) ions are reduced to metallic Pt or Pt(II) ions.

Acknowledgements This work is supported financially by National Natural Science Foundation of China (50373053). We thank Dr. Luo HH for her advice to this paper.

References

1. Goodenough JB, Hamnett A, Kennedy BJ, Manoharan R, Weeks SA (1990) Electrochim Acta 35(1):199
2. Hogarth MP, Munk J, Shukla AK, Hamnett A (1994) J Appl Electrochem 24(1):85
3. Armadi IS, Wang ZL, Green TC, Henglein A, El-Sayed MA (1996) Science 272(5270):1924
4. Huang JC, Sen RK, Yeager E (1979) J Electrochem Soc 126(5):786
5. Giordano N, Passalacqua E, Recupero V, Vivaldi M, Taylor EJ, Wilemski G (1990) Electrochim Acta 35(9):1411

6. Hogarth MP, Hards GA (1996) Platinum Met Rev 40(4):150
7. Matatov-Meytal Yu, Sheintuch M (2002) Appl Catal A: Gen 231:1
8. Zeng HM, Fu RW (1989) Technol Water Treat 15(3):132
9. Chen SX, Zeng HM (2003) Carbon 41(6):1265
10. Chen SX, Xu RM, Zhang XP, Zeng HM (2002) Chinese J React Polym 11(2):108
11. Chen SX, Liu JR, Zeng HM (2005) J Mater Sci 40:6223
12. Gangeri M, Perathoner S, Centi G (2006) Inorgan Chim Acta 359:4828
13. Liu Z, Hong L, Tham MP, Lim TH, Jiang H (2006) J Power Sources 161:831
14. Zheng HT, Li Y, Chen S, Shen PK (2006) J Power Sources 161(1):371
15. Kim S, Park S-J (2006) J Power Sources 159:42
16. Yoshitake T, Shimakawa Y, Kuroshima S et al (2002) Physica B 323:124
17. Shim J-W, Park S-J, Ryu S-K (2001) Carbon 39:1635
18. Antonucci PL, Alderucci V, Giordano N, Cocke DL, Kim H (1994) J Appl Electrochem 24(1):58
19. Coloma F, SepúLveda-Escribano A, Fierro JLG, Rodríguez-Reinoso F (1996) Appl Catal A: Gen 148(1):63